This is an *Accepted Manuscript*, which has been through the Royal Society of Chemistry peer review process and has been accepted for publication.

Accepted Manuscripts are published online shortly after acceptance, before technical editing, formatting and proof reading. Using this free service, authors can make their results available to the community, in citable form, before we publish the edited article. We will replace this *Accepted Manuscript* with the edited and formatted *Advance Article* as soon as it is available.

You can find more information about *Accepted Manuscripts* in the **Information for Authors**.

Please note that technical editing may introduce minor changes to the text and/or graphics, which may alter content. The journal's standard **Terms & Conditions** and the **Ethical guidelines** still apply. In no event shall the Royal Society of Chemistry be held responsible for any errors or omissions in this *Accepted Manuscript* or any consequences arising from the use of any information it contains.

Journal Name

ARTICLE TYPE

Field-induced slow magnetic relaxation of octahedrally coordinated mononuclear Fe(III)-, Co(II)-, and Mn(III)-containing polyoxometalates†

Rinta Sato, Kosuke Suzuki,* Takuo Minato, Masahiro Shinoe, Kazuya Yamaguchi and Noritaka Mizuno*

Herein, we report for the first time polyoxometalate (POM)-based single-molecule magnets with mononuclear transition metal cores. The mononuclear Fe(III)-, Co(II)-, and Mn(III)-containing POMs have successfully been synthesized from a
10 **trivacant lacunary Keggin-type silicotungstate precursor $TBA_4H_6[A$-α-$SiW_9O_{34}]\cdot2H_2O$ (TBA = tetra-n-butylammonium), and the highly distorted octahedral geometries of the incorporated metal cations resulted in the magnetic anisotropies and the single-molecule magnet**
15 **behavior with mononuclear paramagnetic metal ions under the applied dc field.**

Single-molecule magnets (SMMs) have been of considerable interest because of their novel properties and potential applications in high-density magnetic information storages and
20 quantum computation devices.[1] Following the discovery of the SMM behavior of Mn_{12} cluster,[2] most efforts have been devoted to develop multinuclear clusters with large magnetic ground spin states to achieve large energy barrier for magnetic relaxation.[3] In addition, after the first report of slow magnetic relaxation of the
25 mononuclear lanthanoid complex with large magnetic anisotropy by Ishikawa and coworkers,[4] various lanthanoid-based single-ion magnets (SIMs, or SMMs with mononuclear paramagnetic metal ions) have recently been developed.[5] In contrast, transition metal-based mononuclear SMMs have not been reported until last
30 several years. Because orbital angular momentum of transition metal complexes is easily quenched by the ligand fields, design of coordination geometries of transition metal cations is the crucial factor for development of mononuclear SMMs. Therefore, transition metal complexes with low coordination numbers and
35 low symmetries have been designed to achieve large anisotropies required for mononuclear SMMs.[6,7]

Molecular anionic metal-oxide clusters of early transition metals, polyoxometalates (POMs), are attractive materials in numerous fields.[8] We have utilized lacunary POMs as well-
40 defined and controllable coordination ligands for constructing various metal cores with various coordination geometries which display unique catalytic, photocatalytic, and magnetic properties.[9,10] Most importantly, lacunary POMs are promising ligands for designing SMMs because various coordination
45 geometries of the incorporated metal cations can be formed by utilizing the unique properties of the coordination sites, such as multiple hydrogen bonding networks and protonation behavior. In

addition, undesired intermolecular magnetic interactions can be prevented by the bulkiness of POM ligands. Based on the above-
50 mentioned idea, we have successfully developed several SMMs with unique properties by using a divacant lacunary silicotungstate $[\gamma$-$SiW_{10}O_{36}]^{8-}$ as the multidentate ligand; for example, the SMM properties of homo- and hetero-dinuclear lanthanoid cores could be controlled by simply changing the
55 coordination geometries of the lanthanoid cations.[10] Although a few mononuclear lanthanoid-based SMMs[11] as well as various multinuclear SMMs[12] have been reported by using POMs as the macro ligands, there is no report on POM-based transition metal mononuclear SMMs, to the best of our knowledge.

60 Herein, we report for the first time POM-based SMMs with mononuclear transition metal cores. The mononuclear Fe(III)-, Co(II)-, and Mn(III)-containing POMs (I_M) have successfully been synthesized from an organic solvent soluble trivacant lacunary silicotungstate $TBA_4H_6[A$-α-$SiW_9O_{34}]\cdot2H_2O$ (Fig. 1),[13]
65 and the highly distorted octahedral geometries of the incorporated metal cations could be stabilized by intramolecular multiple hydrogen bonding networks (Fig. 2, Fig. S1), resulting in the magnetic anisotropies and the SMM behavior under the applied dc field. It should also be noted that this is the first example of
70 the SMM with the mononuclear octahedrally coordinated Fe(III) complex.

A mononuclear Fe(III)-containing POM (I_{Fe}) was synthesized by the reaction of $Fe(acac)_3$ (acac = acetylacetonato) with two equivalents of the trivacant lacunary silicotungstate $TBA_4H_6[A$-
75 α-$SiW_9O_{34}]\cdot2H_2O$ in the mixed solvent of acetone and water (96/4 v/v) (see ESI† for the detailed procedure). Single crystals of I_{Fe} suitable for X-ray crystallographic analyses were obtained by recrystallization from the mixed solvent of 1,2-dichloroethane

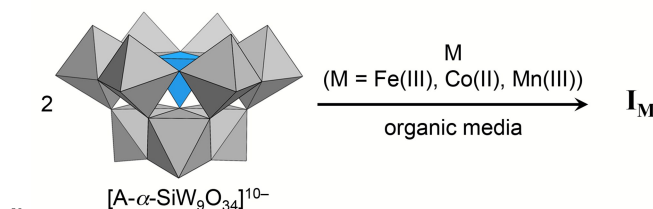**Fig. 1** Schematic representation of the formation of the mononuclear transition metal-containing POMs I_M (M = Fe(III) (I_{Fe}), Co(II) (I_{Co}), and Mn(III) (I_{Mn})) from the trivacant lacunary silicotungstate $TBA_4H_6[A$-α-$SiW_9O_{34}]\cdot2H_2O$ in organic media.
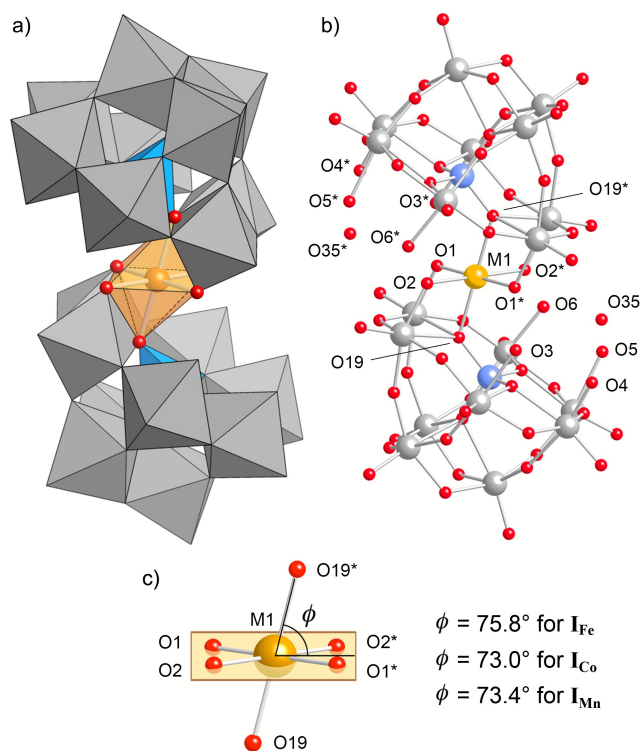
Fig. 2 a) Polyhedral and b) ball-and-stick representations of the anion parts of I_M. Orange, gray, red, and blue spheres represent M (M = Fe(III) (I_{Fe}), Co(II) (I_{Co}), and Mn(III) (I_{Mn})), tungsten, oxygen, and silicon atoms, respectively. c) Schematic representation of the angles (ϕ) between the axial (O19 and O19*) and equatorial oxygen atoms (O1, O2, O1*, and O2*) of the octahedrally coordinated metal cations.

and diethyl ether. Similarly, mononuclear Co(II)- and Mn(III)-containing POMs (I_{Co} and I_{Mn}) were synthesized by using Co(acac)$_2$ and Mn(acac)$_3$, respectively. Single-crystal X-ray analyses revealed that the anion structures of I_{Fe}, I_{Co}, and I_{Mn} were essentially isomorphous S-shaped dimers consisting of one metal cation (Fe(III), Co(II), and Mn(III)) and two sandwiching $[A-\alpha-SiW_9O_{34}]^{10-}$ units (Fig. 2, Fig. S1, Table S1, ESI†). The incorporated metal cations possessed six-coordinate distorted octahedral geometries, and these metal cations were coordinated by four oxygen atoms of W–O (O1, O2, O1*, and O2*) and two axial oxygen atoms of W–O–Si (O19 and O19*) at the lacuna of $[A-\alpha-SiW_9O_{34}]^{10-}$ units. The axial Mn1–O19 and Mn1–O19* coordinations in I_{Mn} were elongated due to the Jahn–Teller distortion (2.223 Å, Table S2, ESI†). Other coordination sites of $[A-\alpha-SiW_9O_{34}]^{10-}$ units remained vacant, and the hydrogen bonding networks between the oxygen atoms of the lacuna were observed; for example, O1···O3*, 2.67 Å; O2···O6*, 2.69 Å; O5···O6, 2.71 Å in I_{Fe} (Fig. 2, Fig. S1, Table S2, ESI†). Additionally, water molecules (O35 and O35*) existed at the lacuna and hydrogen bonding networks were observed between the water molecules and the oxygen atoms (O4, O5, O4*, and O5*) at the lacuna of $[A-\alpha-SiW_9O_{34}]^{10-}$ units. The unique mononuclear transition metal-containing lacunary structures were likely stabilized by these multiple hydrogen bonding networks.

Because of the hydrogen bonding networks and the unique structure of lacuna, the coordination geometries of the incorporated metal cations were considerably distorted from the ideal octahedral geometries. The angles (ϕ) between the axial and equatorial ligands were significantly smaller than 90° (Fig. 2c, 75.8° for I_{Fe}, 73.0° for I_{Co}, and 73.4° for I_{Mn}).[14] These distortions were ideal for large anisotropies required for SMMs. Seven TBA cations were crystallographically assigned in accordance with the results of the elemental analyses. The bond valence sum (BVS) values of W (6.01–6.20), Si (3.94–3.99), Fe (2.90), Co (2.02), and Mn (3.08) of I_{Fe}, I_{Co}, and I_{Mn} indicate that the respective valences are +6, +4, +3, +2, and +3 (Table S3, ESI†). The above-mentioned data of the number of TBA cations and valences of metal cations indicate the presence of ten (for I_{Fe} and I_{Mn}) and eleven (for I_{Co}) protons per each anion. The BVS values of O3 (O3*) (0.53 and 0.50), O5 (O5*) (0.52 and 0.50), O6 (O6*) (0.90 and 0.88) of I_{Fe} and I_{Mn} indicate that protons are located on these oxygen atoms at the lacuna to form the aqua (O3, O5, O3*, and O5*) and hydroxo (O6 and O6*) ligands (Table S3, ESI†). POMs I_{Fe} and I_{Mn} are actually isostructural. The BVS values of O3–O6 (0.70–0.85) of I_{Co} indicate that these oxygen atoms are hydroxo ligands. In addition, the BVS values of O1 and O2 (O1* and O2*) (1.34 and 1.48) of I_{Co} suggest that three out of four equatorial oxygen atoms coordinating to Co(II) are protonated (Table S3, ESI†). The transition metal cations were completely discrete from each other and separated at least by 14 Å due to the bulky $[A-\alpha-SiW_9O_{34}]^{10-}$ ligands and TBA cations, indicating the absence of an undesired intermolecular magnetic exchange pathway.

The cold-spray ionization (CSI) mass spectrum of I_{Fe} in 1,2-dichloroethane showed the two signal sets centered at m/z 6423 and 3333, which agreed well with the simulated patterns for $[TBA_8H_6Fe(SiW_9O_{33})_2]^+$ (m/z 6423) and $[TBA_9H_6Fe(SiW_9O_{33})_2]^{2+}$ (m/z 3333), respectively (Fig. S2, ESI†). Similarly, the CSI-mass spectra of I_{Co} and I_{Mn} showed the signal sets assignable to $[TBA_8H_7Co(SiW_9O_{33})_2]^+$ (m/z 6427) and $[TBA_9HCo(SiW_9O_{31})(SiW_9O_{32})]^{2+}$ (m/z 3307) for I_{Co}, and $[TBA_8H_6Mn(SiW_9O_{33})_2]^+$ (m/z 6422) and $[TBA_9H_6Mn(SiW_9O_{33})_2]^{2+}$ (m/z 3332) for I_{Mn} (Fig. S2, ESI†).

All the above-mentioned results, elemental analyses, and TG-DTA data show that the formulas of I_{Fe}, I_{Co}, and I_{Mn} are $TBA_7H_{10}[Fe(A-\alpha-SiW_9O_{34})_2]\cdot 2H_2O\cdot C_2H_4Cl_2$, $TBA_7H_{11}[Co(A-\alpha-SiW_9O_{34})_2]\cdot 2H_2O\cdot C_2H_4Cl_2$, and $TBA_7H_{10}[Mn(A-\alpha-SiW_9O_{34})_2]\cdot 3H_2O$, respectively ($C_2H_4Cl_2 = $ 1,2-dichloroethane).

The direct current (dc) magnetic susceptibilities of the polycrystalline samples of I_{Fe} and I_{Mn} under the external field of 0.1 T showed that the χT values at 300 K were 4.35 and 3.11 cm^3 K mol^{-1}, respectively, and these values were close to those of the spin-only values for high-spin Fe(III) (4.37 cm^3 K mol^{-1}; $S = 5/2$, $g = 2.00$) and Mn(III) (3.00 cm^3 K mol^{-1}; $S = 2$, $g = 2.00$) (Fig. S3, ESI†). In contrast, the χT value of I_{Co} at 300 K was 2.87 cm^3 K mol^{-1} and larger than the spin-only value for high-spin Co(II) (1.87 cm^3 K mol^{-1}; $S = 3/2$, $g = 2.00$), indicating the presence of considerable contribution of the orbital angular momentum (Fig. S3, ESI†). Upon cooling, these χT values significantly decreased and reached up to the values of 3.58 (I_{Fe}), 1.58 (I_{Mn}), and 1.97 cm^3 K mol^{-1} (I_{Co}) at 1.9 K, indicating the presence of zero-field splitting. Next, low-temperature magnetization data of I_{Fe}, I_{Co}, and I_{Mn} between 1.9 and 10 K were measured under the external fields ranging from 1 to 7 T. The difference in M vs HT^{-1} plots
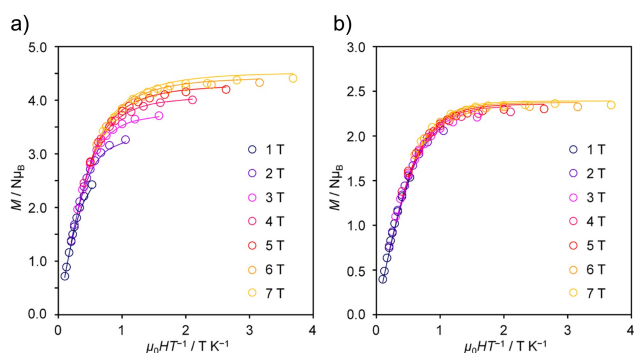
Fig. 3 Low-temperature magnetization data for a) $\mathbf{I_{Fe}}$ and b) $\mathbf{I_{Co}}$ collected in the temperature range of 1.9–10 K under the external field of 1–7 T. Solid lines represent the best fits obtained with PHI program.

under the different external fields indicates the presence of magnetic anisotropy in $\mathbf{I_{Fe}}$ and $\mathbf{I_{Mn}}$ (Fig. 3a and Fig. S4, ESI†). The magnetization data were fitted by using PHI program[15] adopting the anisotropic Hamiltonian (H) given by the following Equation (1) with the parameters of the axial (D) and transverse (E) magnetic anisotropies and isotropic Landé g-factor (g):

$$H = D(S_z^2 - S(S+1)/3) + E(S_x^2 - S_y^2) + \mu_B g\mathbf{SH} \quad (1)$$

The best-fit parameters were as follows: $D = -1.20$ cm^{-1}, $E = 3.41\times10^{-3}$ cm^{-1}, $g = 1.90$ for $\mathbf{I_{Fe}}$; $D = 95.2$ cm^{-1}, $E = 7.18$ cm^{-1}, $g = 2.13$ for $\mathbf{I_{Co}}$; $D = -5.28$ cm^{-1}, $E = 1.19\times10^{-3}$ cm^{-1}, $g = 2.08$ for $\mathbf{I_{Mn}}$. The small differences in the M vs HT^{-1} plots of $\mathbf{I_{Co}}$ were probably due to the large E value (Fig. 3b). The D and E values of $\mathbf{I_{Co}}$ were comparable to those of the previously reported SMMs with octahedrally coordinated Co(II) (Table S6, ESI†).[16] The electron spin resonance (ESR) spectrum (X-band) of the polycrystalline sample of $\mathbf{I_{Co}}$ at 4.2 K showed that g_x, g_y, and g_z values were 3.31, 6.76, and 1.88, respectively (Fig. S5, ESI†). The pattern of g values is characteristic of high spin octahedral Co(II) complexes with positive D values (easy-plane anisotropy), supporting the analysis of the magnetization data.[16–18]

The alternating current (ac) magnetic susceptibilities of $\mathbf{I_{Fe}}$ and $\mathbf{I_{Co}}$ were investigated under the different external dc fields in the range of 0–0.5 T to reveal their SMM behavior (Fig. S6, ESI†). Although negligible out-of-phase signals (χ'') were observed under the zero external dc field probably because of quantum tunneling of magnetization (QTM), peaks of χ'' appeared under the external dc field. Under the external dc field of 0.1 T, the maximum values of the relaxation time were observed. Therefore, the ac magnetic susceptibility measurements were carried out under the external dc field of 0.1 T in the temperature range of 1.9–10 K (Fig. 4). The ac magnetic susceptibilities of $\mathbf{I_{Fe}}$ and $\mathbf{I_{Co}}$ showed the strong temperature- and frequency-dependence and are characteristic of the SMM behavior, indicating the presence of slow magnetic relaxation process. The Cole-Cole plots in the form of χ'' vs in-phase signal (χ') were generated from the ac magnetic susceptibility data and fitted using the generalized Debye model (Fig. S7, ESI†). The α values were in the range of 0.03–0.08 ($\mathbf{I_{Fe}}$) and 0.05–0.07 ($\mathbf{I_{Co}}$), and the small α values support a single relaxation process (Table S4 and Table S5, ESI†,
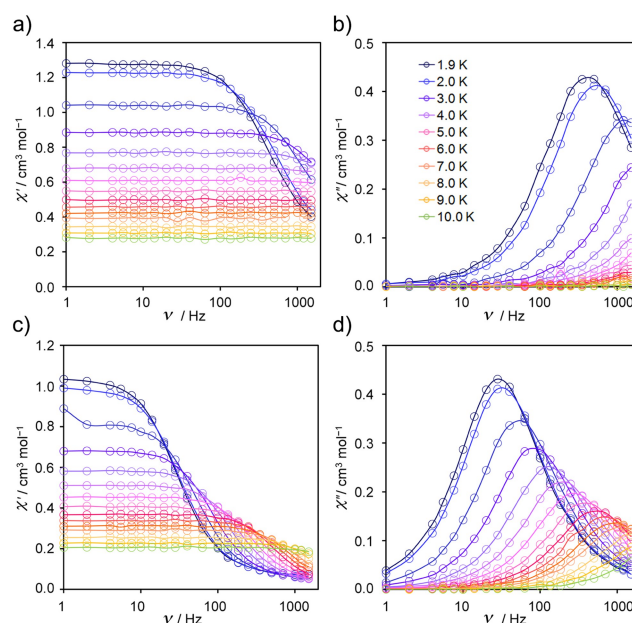

Fig. 4 Frequency dependence of a) χ' and b) χ'' for $\mathbf{I_{Fe}}$, and c) χ' and d) χ'' for $\mathbf{I_{Co}}$ collected in the temperature range of 1.9–10 K under the external dc field of 0.1 T.

α value represents distribution of relaxation times, $\alpha = 0$ for the Debye model). The magnetization relaxation times (τ) were evaluated from the frequency of maxima in χ'' of the frequency dependence of χ'' (Fig. 4), and lnτ values were plotted as a function of T^{-1} (Fig. S8, ESI†). The fit for the Arrhenius equation (lnτ ($\tau = \tau_0$exp(U_{eff}/k_BT)) vs T^{-1}) afforded the parameters of thermal energy barrier for magnetization relaxation (U_{eff}) and pre-exponential factor (τ_0): $U_{eff} = 9.2$ K (6.4 cm^{-1}), $\tau_0 = 3.3\times10^{-6}$ s for $\mathbf{I_{Fe}}$, and $U_{eff} = 19.3$ K (13.5 cm^{-1}), $\tau_0 = 8.2\times10^{-6}$ s for $\mathbf{I_{Co}}$. These results support the SMM behavior of $\mathbf{I_{Fe}}$ and $\mathbf{I_{Co}}$.[16] In addition, the ac magnetic susceptibility of $\mathbf{I_{Mn}}$ showed the temperature- and frequency-dependent χ' and χ'' under the external dc field of 0.1 T, which are characteristic of the SMM behavior (Fig. S9 and Fig. S10, ESI†).[19]

These compounds are the first examples of mononuclear transition metal-containing POMs showing SMM behavior under the applied dc field. In particular, there is no report on SMMs of octahedrally coordinated mononuclear Fe(III) complexes, and it should also be noted that there is only one report on the SMM with the mononuclear Fe(III) complex, to the best of our knowledge.[6e] The transition metals in the POMs reported herein possessed the highly distorted octahedral coordination geometry which breaks the degeneracy of octahedral symmetry, resulting in the large magnetic anisotropy and the SMM behavior with one paramagnetic metal ion.

ChemComm Accepted Manuscript

Notes and references

Department of Applied Chemistry, School of Engineering, The University of Tokyo, 7-3-1 Hongo, Bunkyo-ku, Tokyo 113-8656, Japan. E-mail: ksuzuki@appchem.t.u-tokyo.ac.jp, tmizuno@mail.ecc.u-tokyo.ac.jp; Fax: (+)81-3-5841-7220

† Electronic supplementary information (ESI) available. Experimental details including syntheses, crystallographic data, magnetic susceptibility data, CSI-mass, ESR, IR, and UV-Vis spectra of I_{Fe}, I_{Co}, and I_{Mn}. CCDC reference numbers 1035329 (I_{Fe}), 1035330 (I_{Co}), and 1035331 (I_{Mn}). For ESI and crystallographic data in CIF or other electronic format see DOI: 10.1039/ b000000x/

1   D. Gatteschi, R. Sessoli and J. Villain, *Molecular Nanomagnets*, Oxford University Press, Oxford, UK, 2006.
2   R. Sessoli, D. Gatteschi, A. Caneschi and M. A. Novak, *Nature*, 1993, **365**, 141–143.
3   (*a*) C. J. Milios, A. Vinslava, W. Wernsdorfer, S. Moggach, S. Parsons, S. P. Perlepes, G. Christou and E. K. Brechin, *J. Am. Chem. Soc.*, 2007, **129**, 2754–2755; (*b*) J. D. Rinehart, M. Fang, W. J. Evans and J. R. Long, *Nat. Chem.*, 2011, **3**, 583–542; (*c*) J. D .Rinehart, M. Fang, W. J. Evans and J. R. Long, *J. Am. Chem. Soc.*, 2011, **133**, 14236–14239; (*d*) R. J. Blagg, L. Ungur, F. Tuna, J. Speak, P. Comar, D. Collison, W. Wernsdorfer, E. J. L. Mclnnes, L. F. Chibotaru and R. E. P. Winpenny, *Nat. Chem.*, 2013, **5**, 673–678.
4   N. Ishikawa, M. Sugita, T. Ishikawa, S. Koshihara and Y. Kaizu, *J. Am. Chem. Soc.*, 2003, **125**, 8694–8695.
5   (*a*) S.-D. Jiang, B.-W. Wang, H.-L. Sun, Z.-M. Wang and S. Gao, *J. Am. Chem. Soc.*, 2011, **133**, 4730–4733; (*b*) A. Yamashita, A. Watanabe, S. Akine, T. Nabeshima, M. Nakano, T. Yamamura and T. Kajiwara, *Angew. Chem. Int. Ed.*, 2011, **50**, 4016–4019; (*c*) K. R. Meihaus and J. R. Long, *J. Am. Chem. Soc.*, 2013, **135**, 17952–17957; (*d*) J. J. Le Roy, L. Ungur, I. Korobkov, L. F. Chibotaru and M. Murugesu, *J. Am. Chem. Soc.*, 2014, **136**, 8003–8010; (*e*) L. Ungur, J. J. Le Roy, I. Korobkov, M. Murugesu and L. F. Chibotaru, *Angew. Chem. Int. Ed.*, 2014, **53**, 4413–4417.
6   (*a*) D. E. Freedman, W. H. Harman, T. D. Harris, G. J. Long, C. J. Chang and J. R. Long, *J. Am. Chem. Soc.*, 2010, **132**, 1224–1225; (*b*) W. H. Harman, T. D. Harris, D. E. Freedman, H. Fong, A. Chang, J. D. Rinehart, A. Ozarowski, M. T. Sougrati, F. Grandjean, G. J. Long, J. R. Long and D. J. Chang, *J. Am. Chem. Soc.*, 2010, **132**, 18115–18126; (*c*) P.-H. Lin, N. C. Smythe, S. I. Gorelsky, S. Maguire, N. J. Henson, I. Korobkov, B. L. Scott, J. C. Gordon, R. T. Baker and M. Murugesu, *J. Am. Chem. Soc.*, 2011, **133**, 15806–15809; (*d*) J. M. Zadrozny, D. J. Xiao, M. Atanasov, G. J. Long, F. Grandjean, F. Neese and J. R. Long, *Nat. Chem.*, 2013, **5**, 577–581; (*e*) S. Mossin, B. L. Tran, D. Adhikari, M. Pink, F. W. Heinemann, J. Sutter, R. K. Szilagyi, K. Meyer and D. J. Mindiola, *J. Am. Chem. Soc.*, 2012, **134**, 13651–13661.
7   (*a*) J. M. Zadrozny and J. R. Long, *J. Am. Chem. Soc.*, 2011, **133**, 20732–20734; (*b*) T. Jurca, A. Farghal, P.-H. Lin, I. Korobkov, M. Murugesu and D. S. Richeson, *J. Am. Chem. Soc.*, 2011, **133**, 15814–15817; (*c*) S. Gomez-Coca, E. Cremades, N. Aliaga-Alcalde and E. Ruiz, *J. Am. Chem. Soc.*, 2013, **135**, 7010–7018.
8   (*a*) M. T. Pope, *Heteropoly and Isopoly Oxometalates*, Springer, Berlin, 1983; (*b*) N. Mizuno and M. Misono, *Chem. Rev.*, 1998, **98**, 199–218; (*c*) R. Neumann, *Prog. Inorg. Chem.*, 1998, **47**, 317–370; (*d*) C. L. Hill, in *Comprehensive Coordination Chemistry II* (Eds.: J. A. McCleverty, T. J. Meyer), Elsevier Pergamon, Amsterdam, 2004, vol. 4, pp. 679–759; (*e*) D.-L. Long, R. Tsunashima and L. Cronin, *Angew. Chem. Int. Ed.*, 2010, **49**, 1736–1758; (*f*) K. Kamata, K. Yonehara, Y. Sumida, K. Yamaguchi, S. Hikichi and N. Mizuno, *Science*, 2003, **300**, 964–966.
9   (*a*) K. Suzuki, F. Tang, Y. Kikukawa, K. Yamaguchi and N. Mizuno, *Angew. Chem. Int. Ed.*, 2014, **53**, 5356–5360; (*b*) K. Suzuki, Y. Kikukawa, S. Uchida, H. Tokoro, K. Imoto, S. Ohkoshi and N. Mizuno, *Angew. Chem. Int. Ed.*, 2012, **51**, 1597–1601; (*c*) Y. Kikukawa, K. Suzuki, M. Sugawa, T. Hirano, K. Kamata, K. Yamaguchi and N. Mizuno, *Angew. Chem. Int. Ed.*, 2012, **51**, 3686–3690; (*d*) K. Suzuki, M. Sugawa, Y. Kikukawa, K. Kamata, K.

Yamaguchi and N. Mizuno, *Inorg. Chem.*, 2012, **51**, 6953–6961; (*e*) T. Hirano, K. Uehara, K. Kamata and N. Mizuno, *J. Am. Chem. Soc.*, 2012, **134**, 6425–6433; (f) Y. Kikukawa, K. Yamaguchi and N. Mizuno, *Angew. Chem. Int. Ed.*, 2010, **49**, 6096–6100.
10   (*a*) K. Suzuki, R. Sato and N. Mizuno, *Chem. Sci.*, 2013, **4**, 596–600; (*b*) R. Sato, K. Suzuki, M. Sugawa and N. Mizuno, *Chem. –Eur. J.*, 2013, **19**, 12982–12990.
11   (*a*) M. A. AlDamen, J. M. Clemente-Juan, E. Coronado, C. Martí-Gastaldo and A. Gaita-Ariño, *J. Am. Chem. Soc.*, 2008, **130**, 8874–8875; (*b*) S. Cardona-Serra, J. M. Clemente-Juan, E. Coronado, A. Gaita-Ariño, A. Camón, M. Evangelisti, F. Luis, M. J. Martínez-Pérez and J. Sesé, *J. Am. Chem. Soc.*, 2012, **134**, 14982–14990; (*c*) J. J. Baldoví, J. M. Clemente-Juan, E. Coronado, Y. Duan, A. Gaita-Ariño and C. Giménez-Saiz, *Inorg. Chem.*, 2014, **53**, 9976–9980.
12   (*a*) C. Ritchie, A. Ferguson, H. Nojiri, H. N. Miras, Y.-F. Song, D.-L. Long, E. Burkholder, M. Murrie, P. Kögerler, E. K. Brechin and L. Cronin, *Angew. Chem. Int. Ed.*, 2008, **47**, 5609–5612; (*b*) J.-D. Compain, P. Mialane, A. Dolbecq, I. M. Mbomekallé, J. Marrot, F. Sécheresse, E. Rivière, G. Rogez and W. Wernsdorfer, *Angew. Chem. Int. Ed.*, 2009, **48**, 3077–3081; (*c*) M. Ibrahim, Y. Lan, B. S. Bassil, Y. Xiang, A. Suchopar, A. K. Powell and U. Kortz, *Angew. Chem. Int. Ed.*, 2011, **50**, 4708–4711; (*d*) Y. Sawada, W. Kosaka, Y. Hayashi and H. Miyasaka, *Inorg. Chem.*, 2012, **51**, 4824–4832; (*e*) X. Fang, P. Kögerler, M. Speldrich, H. Schilder and M. Luban, *Chem. Commun.*, 2012, **48**, 1218–1220; (*f*) H. E. Moll, A. Dolbecq, J. Marrot, G. Rousseau, M. Haouas, F. Taulelle, G. Rogez, W. Wernsdorfer, B. Keita and P. Mialane, *Chem. –Eur. J.*, 2012, **18**, 3845–3849; (*g*) M. Vonci and C. Boskovic, *Aust. J. Chem.*, 2014, **67**, 1542–1552.
13   T. Minato, K. Suzuki, K. Kamata and N. Mizuno, *Chem. –Eur. J.*, 2014, **20**, 5946–5952.
14   The angle distortion parameter of Co(II) in I_{Co} was much larger than those of the reported mononuclear SMMs (Table S6, ESI†).[17]
15   N. F. Chilton, R. P. Anderson, L. D. Turner, A. Soncini and K. S. Murray, *J. Comput. Chem.*, 2013, **34**, 1164–1175.
16   There are several reports on octahedrally coordinated mononuclear Co(II) SMMs (SIMs): (*a*) S. Karasawa, G. Zhou, H. Morikawa and N. Koga, *J. Am. Chem. Soc.*, 2003, **125**, 13676; (*b*) J. Vallejo, I. Castro, R. Ruiz-García, J. Cano, M. Julve, F. Lloret, G. D. Munno, W. Wernsdorfer and E. Pardo, *J. Am. Chem. Soc.*, 2012, **134**, 15704–15707; (*c*) E. Colacio, J. Ruiz, E. Ruiz, E. Cremades, J. Krzystek, S. Carretta, J. Cano, T. Guidi, W. Wernsdorfer and E. K. Brechin, *Angew. Chem. Int. Ed.*, 2013, **52**, 9130–9134; (*d*) R. Herchel, L. Váhovská, I. Potočňák and Z. Trávníček, *Inorg. Chem.*, 2014, **53**, 5896–5898; (*e*) S. Gómez-Coca, A. Urtizberea, E. Cremades, P. J. Alonso, A. Camón, E. Ruiz and F. Luis, *Nat. Commun.*, 2014, **5**, 4300.
17   L. Banci, A. Bencini, C. Benelli, D. Gatteschi and C. Zanchini, *Struct. Bond.*, 1982, **52**, 37–86.
18   Because of the large *E* value, accurate determination of the *D* value of I_{Co} will require high field and high frequency ESR measurements.
19   There are several reports on slow magnetic relaxation of mononuclear Mn(III) complexes: (*a*) J. Vallejo, A. Pascual-Álvarez, J. Cano, I. Castro, M. Julve, F. Lloret, J. Krzystek, G. De Munno, D. Armentano, W. Wernsdorfer, R. Ruiz-García and E. Pardo, *Angew. Chem. Int. Ed.*, 2013, **52**, 14075–14709; (*b*) R. Ishikawa, R. Miyamoto, H. Nojiri, B. K. Breedlove and M. Yamashita, *Inorg. Chem.*, 2013, **52**, 8300–8302; (*c*) A. Grigoropoulos, M. Pissas, P. Papatolis, V. Psycharis, P. Kyritsis and Y. Sanakis, *Inorg. Chem.*, 2013, **52**, 12869–12871; (*d*) G. A. Craig, J. J. Marbey, S. Hill, O. Roubeau, S. Parsons and M. Murrie, *Inorg. Chem.*, 2015, **54**, 13–15.

ChemComm Accepted Manuscript